Role of Relaxation on Strain Crystallization of Uniaxially Stretched Poly(ethylene naphthalate) Films: A Mechanooptical Study

C. Martins and M. Cakmak*

Polymer Engineering Institute, University of Akron, Akron, Ohio 44325-0301

Received October 12, 2005; Revised Manuscript Received May 5, 2006

ABSTRACT: The large deformation mechanooptical behavior of amorphous films of PEN in the rubbery temperature exhibits three-regime behavior. Regime I corresponds to classical stress−optical behavior of amorphous materials where PEN remains completely amorphous during stretching. Oriented crystallization and long-range connected network formation accompany the positive slope change in stress−optical behavior into regime II. In the last regime, III, the formation of "muscle bound" structure begins to level off birefringence as it approaches the finite extensibility of polymer chains. Relaxation of uniaxially stretched PEN was found to depend exclusively on the regime from which the relaxation is initiated. If the relaxation is initiated from within regime I, the stress and birefringence decrease traces back the linear stress−optical behavior while the material remains amorphous. The relaxation of stress and birefringence from the early stages of regime II deviates from the linear stress−optical behavior. At long enough relaxation times, birefringence eventually begins to increase while stress continues to decline. This marks the formation of highly localized highly oriented ordered regions with low translational ordering along the chain axis in the material. This unexpected behavior during relaxation was attributed to the formation of a long-range physical network that helps arrest the relaxation of orientations gained during stretching. If the relaxation is initiated toward the end of regime II, a fast increase of birefringence is observed while the stress decreases. This behavior is found to be the result of a spontaneous deformation process as observed by the increase of local true strain in the absence of macroscopic deformation. However, this mechanism is not as a result of relaxation alone but a combination of relaxation coupled with continuation of the deformation process that started during stretching and did not stop when the relaxation process started. In regime III, stress relaxation accompanies little or no increase in birefringence. In regime III other than establishment of three-dimensional order in crystalline regions, no other significant change is observed.

Introduction

During the orientation of polymeric films, relaxation takes place either as a competing mechanism to orientation[1] due to the tendency of molecules to be in the coiled state or purposely induced to increase the stability of the film and avoid shrinkage in certain film applications.[2] The magnitude and rate of stress relaxation depend greatly on processing conditions applied either during the deformation process by affecting the final state of the material or in the relaxation process by affecting the mobility of the chains in the amorphous regions.

The effect of processing conditions on the deformation behavior of PEN films has been investigated;[3−9] however very few studies are reported regarding its relaxation[10] and shrinkage behavior.[11−13]

In the previous paper,[14] the effects of temperature, rate, draw ratio, and molecular weight on the deformation behavior of PEN were investigated. For these studies, on-line measurements of true stress−true strain and birefringence were performed together with the off-line WAXD and DSC measurements to augment the interpretation of structural mechanisms. The stress−optical behavior of PEN was characterized by three regimes that are affected by rate, temperature, and molecular weight. Molecular organizational mechanism responsible for each regime was identified: In regime I, the SOR is followed and the material remains amorphous. With increasing strain, the material rapidly crystallizes through a process of spontaneous deformation. This is defined as regime II, where a fast increase of birefringence accompanies small changes in the stress. The transition between regimes I and II, where the stress−optical rule becomes nonlinear, defines the starting point for the formation of a network that develops very rapidly throughout regime II. When the network starts to tighten, strain hardening occurs and eventually full extensibility of the network occurs. This occurs in regime III, where the birefringence changes are insignificant compared to the stress rise.

Ito et al.[10] investigated the effect of temperature and rate on the relaxation behavior of PEN using on-line measurements of stress and birefringence in simultaneous biaxial mode. They observed that stress relaxation is accompanied by a decrease in birefringence for the rates ($0.1-1\ s^{-1}$) and temperatures (150−170 °C) investigated. However, stress relaxation did not trace back the behavior observed during initial stretching stage.

The deformation effect on PET investigated by Ryu et al.[15] and Ito et al.[10] indicates that for low levels of deformation, where the stress−optical rule (SOR) is applied, the relaxation proceeds by a decrease in birefringence and stress following the same straight line as in the stretching process. At intermediate levels of strain, while Ito et al.[10] observed an increase of birefringence, explained by a process of spontaneous deformation, Ryu et al.[15] show first a decrease in birefringence that then start to increase while the stress relaxes. The change in birefringence was defined as the beginning of strain-induced crystallization. Finally, at high draw ratios, the birefringence increases during the whole period of stress relaxation.

Pearce et al.[16] investigated the effect of temperature on the relaxation behavior of PET by means of infrared spectroscopy. They show that for substantial relaxation to occur temperatures need to be close to the glass transition. However, once the strain hardening occurs, the relaxation is suppressed.

Oultache et al.[17] investigated both the effect of temperature (80−105 °C) and rate (25−100 mm/min) on the orientation and

* Corresponding author. E-mail: Cakmak@uakron.edu.

10.1021/ma0522155 CCC: $33.50
Published on Web 06/08/2006

relaxation of PET by birefringence and infrared spectroscopy techniques. The samples were stretched to a maximum stretch ratio of 2, corresponding to an intermediate level of deformation. When the relaxation starts, stress sharply decreases, and this is followed by a rapid leveling off into a quasi-plateau behavior at longer relaxation times. The increase of temperature or strain rate accelerates the initial relaxation process. The increase in temperature enhances the mobility of the chains. At fast rates, the orientation mechanism dominates the relaxation, and therefore, higher orientation levels are achieved. As soon as the deformation is stopped, there is an elastic driving force that helps the fast recovery of the chains to its random coiled state, resulting in the rapid initial relaxation process. Matthews et al.[18] reported similar studies on PET relaxation from the oriented state.

Stress-induced crystallization has been identified as a primary mechanism to suppress orientation relaxation by a number of researchers.[16,18−21] Once it occurs, the crystals formed act as physical cross-link points, anchoring the molecules in a network hindering the chains from relaxing and recovering their original random coiled state.

The relaxation behavior of PEN films from preoriented state has not been investigated. The present work aims to clarify the structural mechanisms including formation of long-range physical network involved during relaxation of PEN after stretching to three stress−optical regimes. The molecular weight effect will be also investigated as a complementary study to the relaxation behavior of PEN, since it is a parameter that influences the chain length and thus entanglement density.

Experimental Procedures

Materials. Two commercial grades of PEN films with intrinsic viscosity (IV) of 0.54 and 0.67 dL/g were used in this investigation. For convenience, the former is designated by LPEN (lower molecular weight PEN) and the latter by HPEN (high molecular weight PEN). Both films were kindly provided by M&G Polymers Co.

As-received melt cast samples were essentially amorphous (∼5% crystallinity) and exhibited T_g at 120 °C and T_m at 270 °C. The cold crystallization peak depends on the molecular weight of the material, occurring at 190 °C for LPEN and 200 °C for HPEN, indicating slight suppression of crystallization during heating due to increase chain lengths in HPEN.

On-Line Birefringence and True Mechanical Behavior Measurements. A uniaxial stretching machine developed in our group was used to simultaneously determine the mechanooptical properties of PEN films during deformation and relaxation processes. The machine is composed of three parts: the uniaxial stretching machine with environmental chamber, the spectral birefringence system, and a laser-based width measurement system. By a specially designed uniaxial stretching machine allowing the crossheads to move in opposite direction and the use of dumbbell-shaped samples, one guarantees the measurements to be made always in the same stationary midsection of the sample. Therefore, measurements of optical retardation and sample width at the stationary midsymmetry plane and force are recorded simultaneously. Assuming (1) simple extension ($D_t/D_0 = W_t/W_0$) and (2) incompressibility ($L_0W_0D_0 = L_tW_tD_t$), time variation of the local thickness is calculated, and thus birefringence, local true stress, and local true strain are determined. Birefringence measurements were taken at 546 nm wavelength.

$$\text{thickness } D_t = (W_t/W_0)D_0$$

$$\text{birefringence} = \Gamma/D_t$$

$$\text{true strain} = L_t/L_0 - 1 = (W_0/W_t)^2 - 1$$

$$\text{true stress} = F_t/(W_tD_t) = F_t/[(W_t^2/W_0)D_0]$$

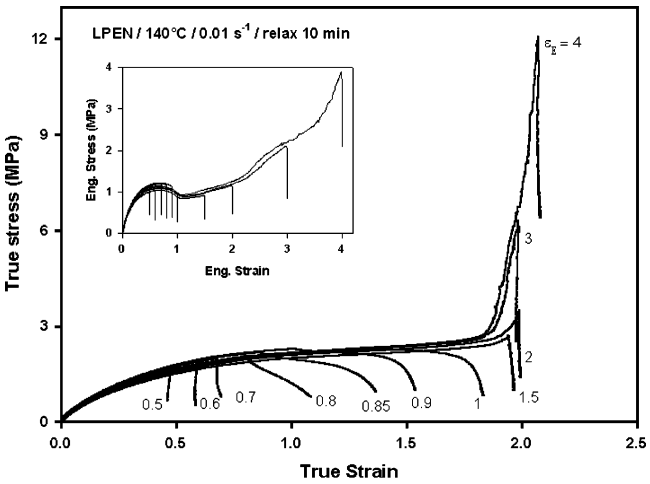

Figure 1. True mechanical behavior of PEN during stretching and relaxation processes. Samples were stretched between 50 and 400% at 140 °C and 0.01 s^{-1} and relaxed for 10 min. In the inset engineering mechanical behavior is presented.

where Γ is the retardation, W_0 and D_0 are the initial width and thickness, and F_t, W_t, and D_t are time variation of force, width, and thickness, respectively.

True strain rate was calculated from true strain vs time curves.

Additional details of the system can be found elsewhere.[22−26] The birefringence measurements taken in this study are all for 546 nm wavelength.

Sample Preparation and Experimental Conditions. Samples of dumbbell shape were cut from the as-cast amorphous film rolls. The dimensions used were 75 mm long, 40 mm wide, and 30 mm wide in the narrowest region. The samples were clamped and mounted on the uniaxial stretching system inside an environmental chamber. The distance between clamps was 30 mm. A period of 10 min was used for equilibration of the sample temperature. The samples were uniaxially stretched at 140 °C and with a rate of 20 mm/min to a series of stretch ratios up to 5×. One set of samples was simply stretched at the conditions mentioned above, and another was allowed to relax for a fixed period of time at the same temperature as applied during stretching. Different relaxation times were used for detailing the structural mechanisms involved in this process. The relaxation step was carried out up to a maximum of 2 h.

Thermal Characterization. Thermal properties of PEN films were measured using a 2920 MDSC V2.6A TA Instruments. The samples of approximately 6−10 mg were scanned at heating rate of 10 °C/min in a dry nitrogen atmosphere. The thermal properties are referred to the maximum peak position. The degree of crystallinity was determined using eq 1, considering the heat of fusion of 100% crystalline (ΔH_f°) to be 103.4 J/g.[27]

$$\chi\,(\%) = \frac{\Delta H_m - \Delta H_c}{\Delta H_f^\circ} \times 100 \qquad (1)$$

ΔH_m and ΔH_c are respectively the enthalpy of melting and enthalpy of crystallization estimated by the DSC curves.

X-ray Measurements. A Bruker AXS generator equipped with a copper target tube and two-dimensional detector was used to obtain the one-quadrant WAXD patterns of the specimens. The generator was operated at 40 kV and 40 mA with a beam monochromitized to Cu Kα radiation. A sample-to-detector distance of 11.5 cm was used for all experiments. A typical exposure time of 10 min was used.

Results and Discussion

Mechanical Behavior. In Figure 1, the true mechanical behavior of LPEN during the process of stretching and relaxation is presented. The samples were stretched to different levels of

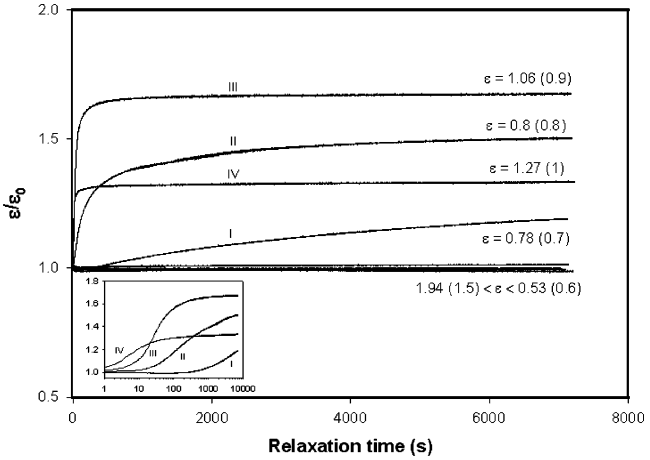

Figure 2. Normalize true strain as a function of relaxation time for LPEN relaxed at 140 °C for 2 h. The values indicate the true strain and engineering strain (in parentheses) at relaxation time zero.

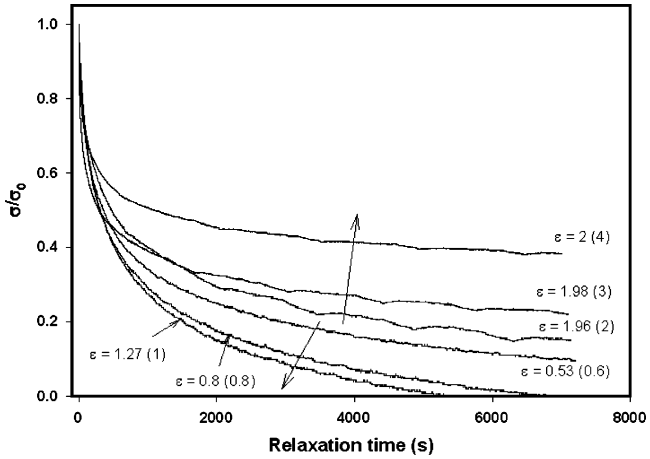

Figure 3. Normalized true stress as a function of relaxation time for LPEN relaxed at 140 °C for 2 h. The values indicate the true strain and engineering strain (between parentheses) at relaxation time zero.

strain and allowed to relax for a period of 10 min at 140 °C (at the stretching temperature). As expected, a stress drop is observed during relaxation of PEN.

However, the stress relaxation is accompanied by an increase in true strain at intermediate levels of deformation. This spontaneous deformation has also been observed by Biangardi and Zachmann[28] and Peszkin et al.[29] while investigating the effects of heat treatment of spun PET fibers.

When the engineering properties are considered (see inset in Figure 1), the stress drops at constant strain, and thus a spontaneous deformation mechanism cannot be observed. The comparison between the true and engineering behaviors shows that the increase of true strain is more pronounced for samples deformed between 80% and 100%, which corresponds to the region of neck formation for PEN.

In Figure 2, the change of strain is plotted as a function of relaxation time. The strain is normalized relative to the strain at relaxation time zero (ϵ/ϵ_0), so that comparison between the samples stretched to different strain levels could be made. A relaxation period of 2 h is shown in this figure.

Three different tendencies are observed: (i) no change in the true strain, as indicated by the unity value of ϵ/ϵ_0, occurring for deformations that are either very low (below 60%) or very high (above 150%); (ii) slow increase of strain through all the relaxation period, as observed for 70% strains; and (iii) rapid increase of stain at beginning of relaxation which slows down and maintains a constant level until the end of relaxation. This last case corresponds to deformations between 80% and 100%, where considerable spontaneous deformation is observed.

As depicted in the inset of Figure 2, where the same plot is represented on a logarithmic scale, the higher the strain applied to the material (I, 70%, ..., IV, 100%), the quicker is the strain increase during relaxation and the sooner is the leveling off of the strain at a constant value. About 200 s is needed for the strain to start increasing when a 70% strain is applied during stretching. The magnitude of strain change increases with the increase of strain from 70% to 90% but is less at 100%.

Figure 3 shows the normalized stress (σ/σ_0) as a function of relaxation time. As observed, the rate of stress relaxation is very fast at the initial stages and tends to level off as the relaxation time increases. The magnitude and rate of stress relaxation at long times depend on the strain applied to the material. The following is observed: as the strain applied to the material increases to 100%, so does the magnitude and rate of stress relaxation, above which a change in this tendency is observed,

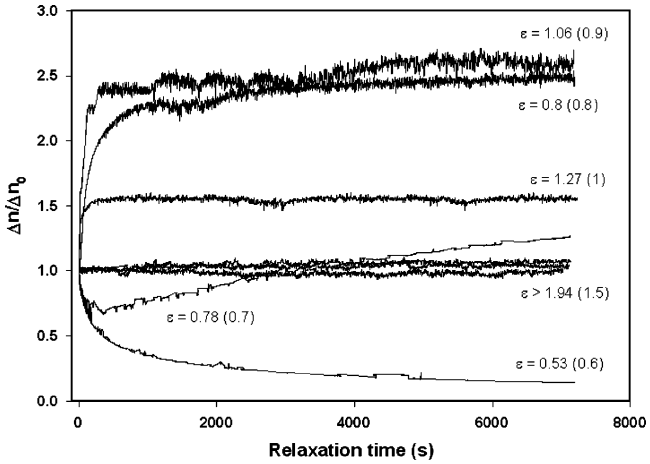

Figure 4. Normalized birefringence as a function of relaxation time for LPEN relaxed at 140 °C for 2 h. The values indicate the true strain and engineering strain (in parentheses) at relaxation time zero.

and the magnitude of stress relaxation decreases with further increase of initial strain. Spontaneous deformation is perhaps the mechanism causing the former behavior, whereas the latter is attributed to strain hardening, as observed by other authors.[16,18−21]

Optical Behavior. While stress relaxation is taking place, considerable change in birefringence is observed in the material. This depends primarily on the applied strain. These results are represented in Figure 4, where the normalized birefringence ($\Delta n/\Delta n_0$) is plotted as a function of relaxation time.

Starting from low prestretching levels, (strain = 60%), the birefringence decreases very fast at the beginning and then slows down as the relaxation time increases. At 70% strain, the birefringence first decreases and then starts increasing slowly. The increase of birefringence starts around 350 s and eventually crosses over the initial birefringence value at around 3200 s. The turnaround of birefringence as well as its slow increase fits with the strain behavior observed previously in Figure 2 where the strain was shown to increase very slowly at 200 s.

This links the increase observed in birefringence to additional deformation that occurs during relaxation as a result of spontaneous deformation. The same is observed between 80% and 100% strains, where birefringence and strain have the same behavior (see Figure 2). Both values increase very rapidly at low relaxation times, reaching a maximum and maintaining there values thereafter. For strains above 150%, no change in

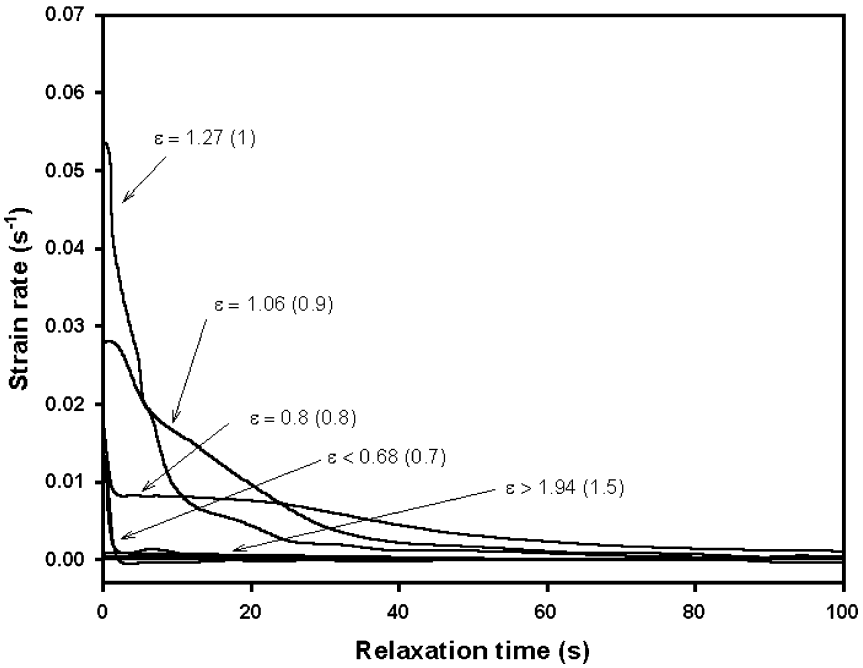

Figure 5. Change of strain rate during relaxation of LPEN at 140 °C. The values indicate the true strain and engineering strain (in parentheses) at relaxation time zero.

birefringence is observed. This is consistent with the strain result that does not change during relaxation after having been stretched to these levels.

Strain Rate. To understand the origin of the spontaneous deformation process during relaxation, the true strain rate was plotted as a function of relaxation time (Figure 5). The strain rate does not reach zero level during relaxation after stretching to intermediate deformation levels. These results explain why there is a very fast increase of strain and birefringence at strains between 80 and 100%, while stress relaxation is taking place. However, the strain rate at 70% does not explain the slow increase in the strain at long times, nor the change in tendency of birefringence, as discussed previously. This result points to a process of spontaneous deformation starting during relaxation and not during stretching, as in the other cases.

For strains less than 70%, the strain rate drops rapidly from the initial set point (strain rate of 0.01 s^{-1}) to zero. At strains between 80% and 100%, the strain rate decreases slowly with time, until it eventually becomes zero. The higher the strain applied to the material during stretching, the faster is the decay of strain rate during relaxation and the shorter is the time needed for it to decrease to zero. For samples stretched above 150% the stain rate is null throughout all the relaxation period and thus so does the strain and birefringence, as plotted in Figures 2 and 4.

The large values of the strain rate observed at intermediate levels of deformation are a result of the spontaneous deformation mechanism developing during stretching, as is shown in Figure 6.

During the start of stretching with a constant engineering strain rate of 0.01 s^{-1}, the monitored true strain rate matches this engineering value for a period of first 45 s, indicating that material deforms affinely. Following this stage, a rapid rise in the true strain rate signifies the occurrence of spontaneous deformation. In the last stage the strain rate measured in the midsection of the sample rapidly approaches zero as it strain hardens and eventually stops deforming. This is shown in detail in Figure 6.

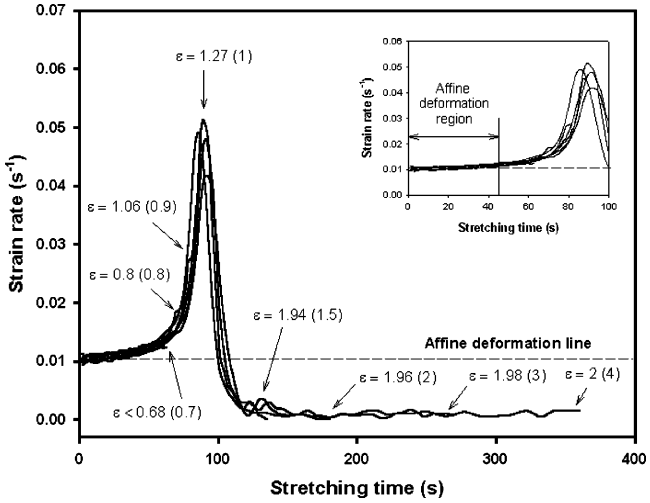

Figure 6. Change of strain rate during stretching of LPEN at 140 °C and 0.01 s^{-1}. The values indicate the true strain and engineering strain (in parentheses) at relaxation time zero.

The arrows in the figure points to the end of the stretching process for samples deformed to different levels of strain. If the stretching process is stopped before the increase of strain rate takes place, the strain rate decreases instantaneously to zero during relaxation, as shown in Figure 5. On the other hand, stopping the stretching process anywhere along the peak (as in the case of strains between 80% and 100%), the relaxation accompanies deformation, which in turn increases birefringence as discussed earlier. As revealed in the previous paper,[14] a very fast increase of birefringence is observed when spontaneous deformation takes place, and as soon as this deformation ceases, the birefringence levels off to a constant level. The latter behavior is observed when the sample is stretched to strains above 150%, in which the strain rate reaches zero and thus no longer changes during the relaxation process.

Mechanoooptical Behavior. In a previous paper,[14] three distinct regimes were identified in mechanooptical behavior of PEN. They were regime I, where the stress−optical rule applies; regime II, where a fast increase of birefringence is observed at

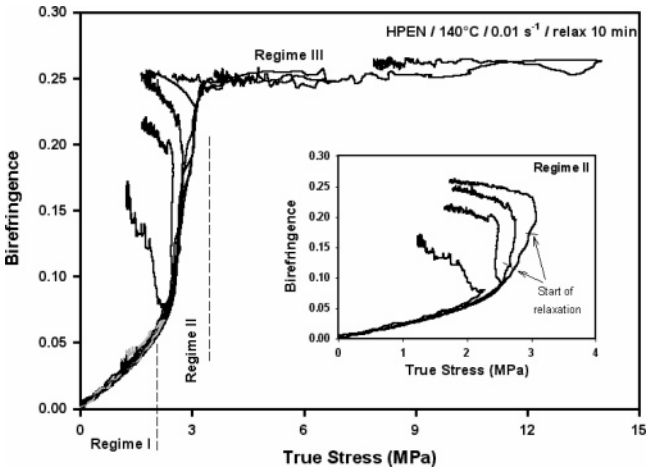

Figure 7. Mechanooptical behavior of LPEN during stretching and relaxation processes. Samples were stretched between 50 and 400% strain at 140 °C and 0.01 s^{-1} and relaxed for 10 min.

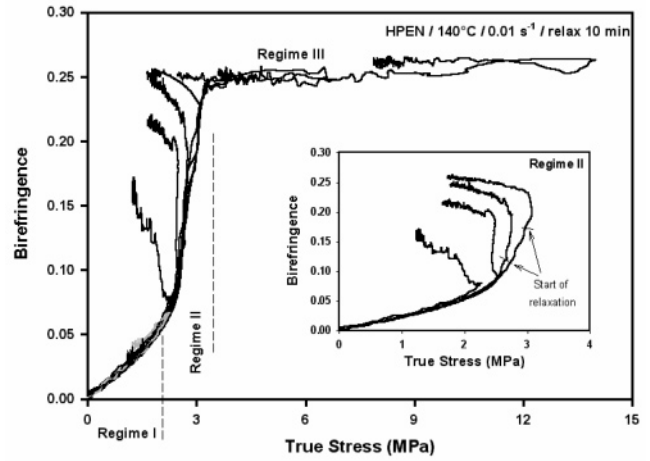

Figure 8. Mechanooptical behavior of HPEN during stretching and relaxation processes. Samples were stretched between 50 and 400% strain at 140 °C and 0.01 s^{-1} and relaxed for 10 min.

almost constant stress as a result of spontaneous deformation; and regime III, where birefringence reached a plateau while the stress continues to increase. Those regimes are now defining substantial differences in the relaxation behavior of PEN, as is shown in Figure 7 for LPEN and in Figure 8 for HPEN, relaxed for 10 min.

Both figures show that when PEN is stretched to strain levels within regime I, the relaxation stage involves the decrease in both stress and birefringence tracing back the same straight line of linear stress−optical behavior recorded during stretching stage. Once the samples are stretched beyond regime I into the early part of regime II, the relaxation stage still involves decreases in both birefringence and stress, but they no longer trace back the slope of regime I as they deviate from it following slower decline in birefringence as the stress decreases. This decline is not indefinite, and at a critical point, the birefringence−stress curve shows a minimum beyond which the birefringence starts to increase. The higher the birefringence attained during the stretching stage, the faster is the increase of birefringence during relaxation. In the transition between regime II and III, the birefringence still increases but not as significantly as in regime II. Finally, when regime III is reached, the birefringence remains nearly constant while stress relaxation proceeds. Ryu et al.[15] and Ito et al.[10] showed similar behaviors during the relaxation behavior of PET. However, the limited investigations on PEN's relaxation behavior, performed by Ito et al.,[10] revealed only a decrease in birefringence not proportional to the stresses. The difference in behavior might be attributed to the high temperatures used in their study (160 °C).

Relaxation behavior in regime II is characterized by the following birefringence changes: (i) decrease of birefringence does not follow back the same curve observed during stretching (70% strains); (ii) birefringence remains constant for a short period, then increases very rapidly, and finally slows down (80−90% strains); (iii) continuous birefringence increase right after ceasing the stretching, decreasing its rate as the relaxation proceeds (100% strains). The changes observed in (ii) and (iii) are related to the strain rate (Figure 5), since the lower the strain rate applied, the slower the birefringence change observed in regime II.

The main impact of the molecular weight on the relaxation behavior was observed in the transition between regimes I and II. For HPEN stretched at 70% strains, the birefringence increases right after the relaxation starts, whereas for LPEN, the birefringence decreases. This slight difference is explained by the differences in efficiency of orientation of the two materials as the entanglement density in HPEN is higher.

A gray line is used in both Figure 7 and Figure 8 to help clarify the deviation from linearity of the stress−optical rule. In Figure 7, the sample that remains in regime I during the stretching traces back the same line during relaxation (note the gray line behavior). The deviation is noted as the initial deformation increased toward regime II where the stress−birefringence relationship becomes nonlinear and before fast spontaneous deformation takes place. This is observed at 70% strains for LPEN (Figure 7). From these results it is possible to conclude that when the material is stretched to a birefringence level between 0.05 and 0.07, the relaxation proceeds with a decrease in stress and birefringence that deviates from from the linearity observed during stretching. Moreover, on the basis of the results shown in Figure 2 (see 70% strains), a very slow increase of strain should be expected within this region of deformation (transition between regimes I and II). The lower the birefringence level attained (within the 0.05−0.07 range), the longer should be the time for the strain to start to increase and the slower the strain increase thereafter.

Structural Studies. To understand the structural changes occurring in the material upon relaxation, WAXD and DSC techniques were applied to both as-stretched and relaxed samples. Figure 9 shows the mechanooptical behavior of LPEN with corresponding WAXD patterns before and after relaxation.

When low strains are applied to LPEN within regime I, the material remains in the amorphous state throughout the deformation and relaxation stages.

In the transition of regimes I to II (strains of 70%), although the material is amorphous before relaxation, a very sharp crystalline peak corresponding to α(010) reflection appears. This means that uniplanar axial texture is developing at very early stages of deformation. It is important to note that this peak represents those regions that exhibit near perfect orientation along the stretching direction despite the fact that it is observed during relaxation stage that should have led to low orientation levels. Because the off-equatorial peaks are not present in this pattern, the regions exhibiting near perfect orientation exhibit low translational ordering along the stretching direction. When deformation reaches 80% strain, the amorphous material converts to a crystalline structure of low orientation and low three-dimensional order (poor interchain registry along the chain axis) since the off-equatorial peaks are only slightly defined.

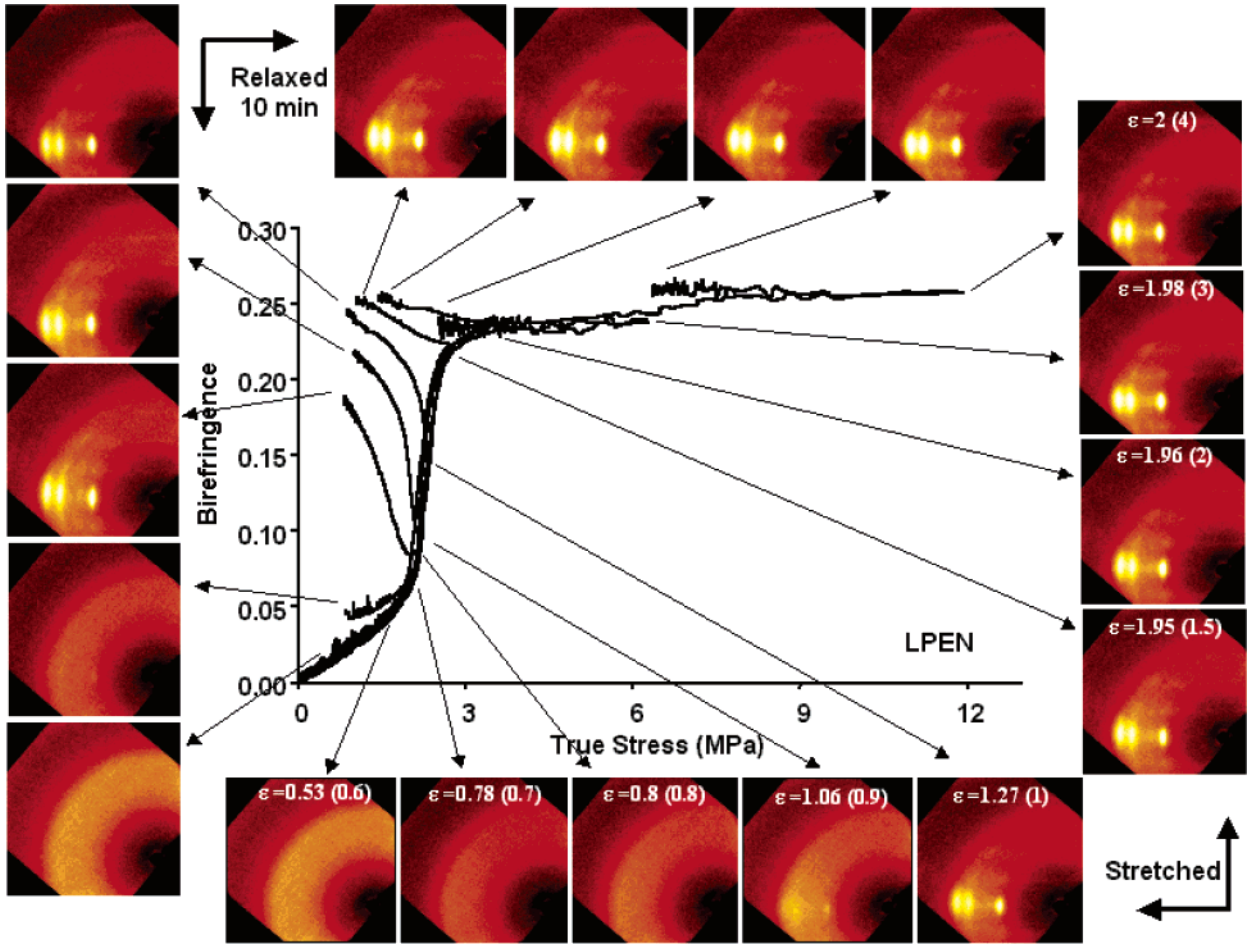

Figure 9. Mechanooptical behavior of LPEN during stretching and relaxation processes with corresponding WAXD pattern. Samples were stretched at 140 °C and 0.01 s^{-1} and relaxed for 10 min. The values indicated in the pictures are referring to the true strain and engineering strain (in parentheses) at relaxation time zero.

In this case, reflections of α(010), $\beta(\bar{2}20)$, α(100), and α-$(\bar{1}10)$ planes can be clearly seen. At 90% strains, crystalline reflections of the α(010) plane can be distinguished together with a broad peak where reflections of α(100) and α$(\bar{1}10)$ are expected to appear. From this state, the material develops a crystalline state of higher crystalline perfection but of lower crystalline orientation. At strains of 100% the starting structure is already crystalline but with low three-dimensional ordering. With further relaxation, the interchain registry improves, but not significantly.

Throughout regime III, as the strain applied to the material increases, the ordering of the material also increases, so in the relaxation stage only slight crystalline disorientation is detected.

In Figure 10 and Figure 11 the DSC thermograms and percentage of crystallinity of both LPEN stretched and relaxed samples are presented.

Comparing only the as stretched samples, it is observed that (i) the glass transition temperature increases and its region broadens as the strain is applied to the material especially above 100%; (ii) the cold crystallization temperature (T_{cc}) decreases, and the area under its peak changes considerably as the strain increases. For example, with only 50% strain, the peak position of T_{cc} moves 6 °C below its original position (190 °C). T_{cc} is maintained at this position until about 70% strain; however, broadening of this peak occurs while the crystallinity remains below 10% during this period (Figure 11). It is important to recall that the sample stretched with 60% strain is within regime I, and with 70% it is in the nonlinear transition region between regimes I and IIa. At 80% strain, the sample is at the start of regime II. And at this condition T_{cc} decreases 13 °C to 177 °C, and a lower temperature shoulder appears in the cold crystallization peak. This signifies the development of two distinct chain populations of differing orientation levels.

The lower peak corresponds to the chain population that possesses higher orientation and higher peak correspond to those amorphous chains with low orientation levels. This also suggests that the overall structure becomes inhomogeneous with regions of higher orientation and regions of lower orientation. The crystallinity is around 13% (by DSC) at this stage of deformation, which translates into an amorphous WAXS pattern as depicted in Figure 9, indicating that this level of crystallinity is simply as a result of overall "uniform compaction" of the structure and does not represent 13% of the material possessing 100% crystallinity. At 90% strain, the T_{cc} moves again, being in the position of the T_{cc} of the more oriented population. The crystallinity increases from 13% to 20%. Above 100% strains, a considerable shift of T_{cc} and reduction of its peak area are observed and as a result of strain hardening of the material, where PEN reaches a plateau with crystallinity around 38%.

When relaxation takes place within regime I (below 60% strains), no change is observed in the peak and area of T_{cc}. Consequently, the crystallinity level remains constant at around 8% after relaxation, reflecting an effectively amorphous state of the material shown by WAXD. At the start of regime II around 70% strains (point I marked in Figure 11), the crystallinity slightly increases from less than 10% to 13% on 10 min relaxation, reflecting the decrease of T_{cc} observed in Figure 10. Like the samples stretched at 80%, a bimodal population appears

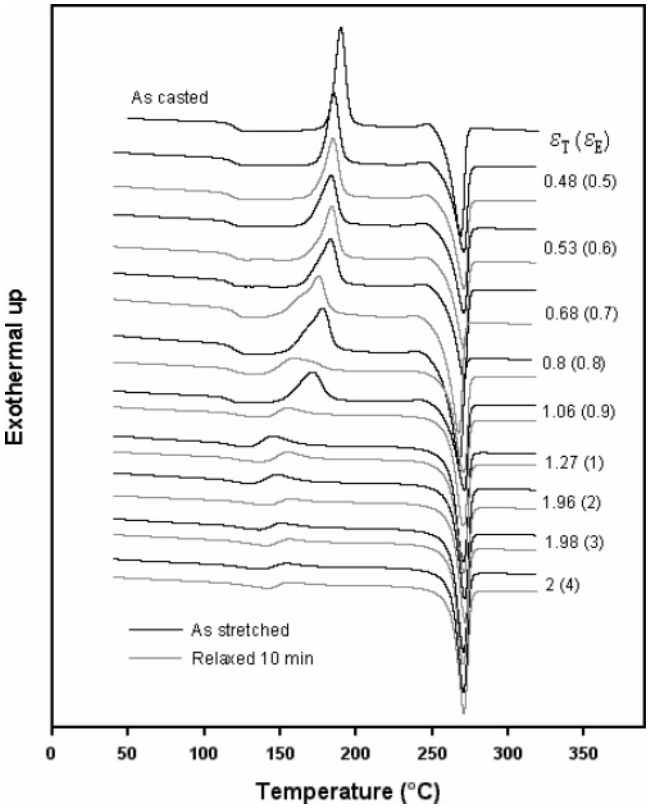

Figure 10. DSC thermograms of LPEN samples stretched at different strains at 140 °C and 0.01 s^{-1} and relaxed for 10 min at 140 °C. The values indicate the true strain and engineering strain (in parentheses) at relaxation time zero.

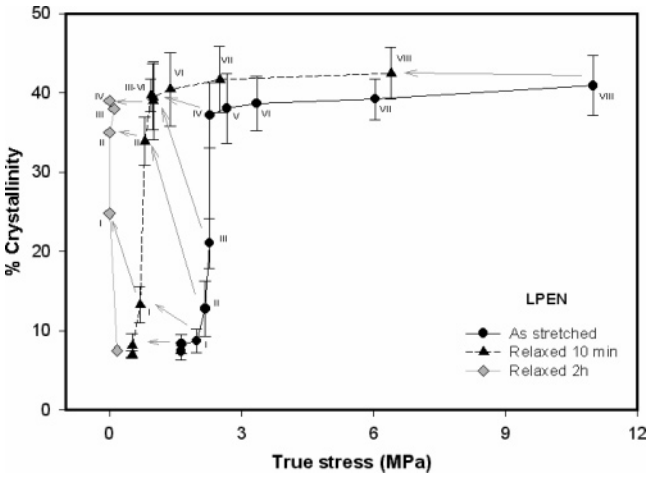

Figure 11. Percentage of crystallinity of LPEN as stretched and relaxed samples as a function of true stress. Samples were stretched to strains between 50 and 400% at 140 °C and 0.01 s^{-1} and finally relaxed for 10 min and 2 h. The numbers identify the as stretched and relaxed pairs. Number I corresponds to 70%, II to 80%, ..., and VIII to 400%. No number was indicated below 60%.

during relaxation, showing that the same kind of structure can be formed either during stretching or during relaxation. Both of them show similar WAXD patterns of a near perfectly oriented structure of low translational order along the chain axis, resembling a nematic-like structure. Despite the increase in crystallinity, birefringence decreases (Figure 9), indicating that substantial amorphous chain relaxation must be occurring simultaneously with crystallization, the former being more dominant than the latter. Relaxation of samples stretched at 80% causes a decrease of T_{cc} to around 156 °C, which is maintained for the relaxed samples that have been strained to higher levels.

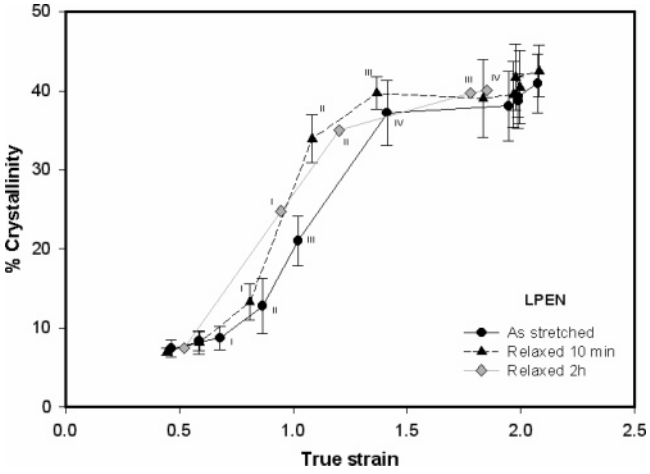

Figure 12. Percentage of crystallinity of as stretched and relaxed samples as a function of true strain. Samples were stretched to different levels of strains between 50 and 400% at 140 °C and 0.01 s^{-1} and finally relaxed for 10 min and 2 h.

The area under the peak also reduces upon relaxation, reducing even further during relaxation at 90% strains, after which no significant change is observed. The crystallinity of the relaxed material increases to around 35% and 40% respectively for 80 and 90% strains (points II and III). Thus, relaxation within regime II causes substantial chain orientation (reduction of T_{cc}) and crystallization (reduction of T_{cc} peak area) as a result of the spontaneous deformation mechanism, therefore explaining the increase of birefringence in Figure 9. Above 100% strain, the T_{cc} of the relaxed samples moves to slightly higher temperatures, appearing in the same position as in the samples simply stretched at 400% strains, whereas the area under the peak is reduced slightly as the strain increases. This corresponds to very small 3% increase in crystallinity.

In Figure 12, the crystallinity of as-stretched and relaxed samples is plotted as a function of true strain. When the material is strained at 70% (point I), the crystallization increases during relaxation accompanied by an increase of strain. The same occurs at 80% strain (point II) and to some extent at 90% strain (point III). In this last case, the crystallinity level increases substantially after 10 min relaxation but does not change thereafter. The increase of crystallinity is due to the increase of strain shown to occur as a result of the spontaneous deformation during stretching and relaxation. Above 100% strains (point IV), no change in crystallinity is observed.

Figure 12 shows that as the strain increases the crystallinity first increases slightly as the strain increases to about 0.7, and then at intermediate true strains (between 0.7 and 1.4) the crystallinity increases very rapidly, from less than 10% to 38−40%. Finally it levels off at 40−42%.

The development of crystallinity is governed by the strain applied to material. This can occur either during the stretching stage or as a spontaneous deformation during relaxation stage. The latter is typically observed after stretching to intermediate deformation levels. Once strain hardening occurs, very small change in the true strain is observed; hence, the saturation behavior observed at the high strain end of the plot.

Relaxation at intermediate states of deformation (relaxation within regime II) accompanies substantial structural changes. To detail the structural evolution mechanism in this regime during relaxation, different relaxation times were further applied and investigated. The results are shown in Figures 13−16.

Figure 13 details the structural changes occurring during 2 h relaxation after a 70% strain has been applied to the material.

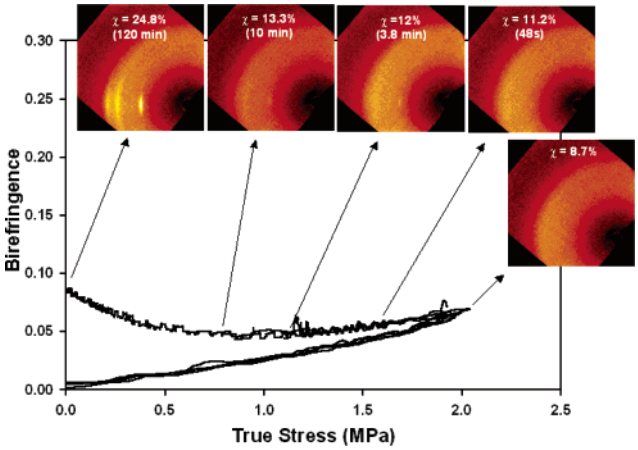

Figure 13. Detailed mechanooptical behavior and WAXD patterns of LPEN strained at 70% and relaxed for 2 h.

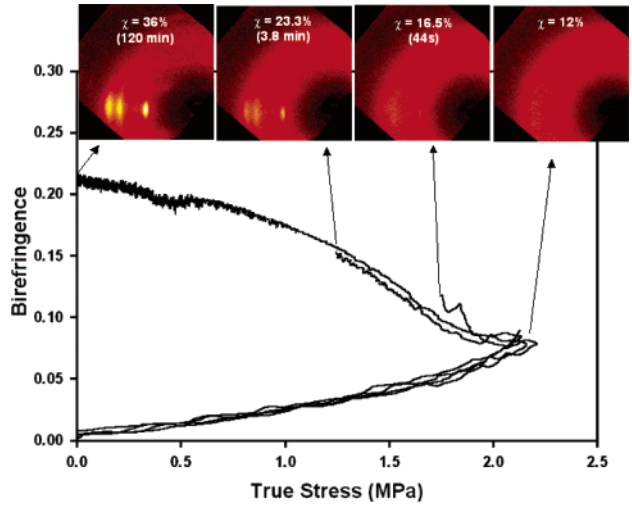

Figure 14. Detailed mechanooptical behavior and WAXD patterns of LPEN strain at 80% and relaxed for 2 h.

The decrease of birefringence in the first 4 min is accompanied by the appearance of extremely sharp equatorial peak of α(010). Following the appearance of this peak, the birefringence levels off for a while (about 6 min) while the stress relaxation continues. A crystalline structure with relatively low orientation and no three-dimensional ordering is formed, as seen by the absence of off-equatorial peaks in the WAXD pattern.

At 2 h relaxation, the azimuthal distribution of the crystalline peaks begin to increase, indicating that the crystallization that is occurring as part of the long-term relaxation process involves reduction in crystalline orientation. The most likely reason for this is the crystallization of polymer chains which has relaxed to a certain extent during this process.

An important conclusion in this structural organizational process is that the nearly perfectly oriented regions form throughout the body of the material and these regions must somehow be connected to each other through a three-dimensional network that is rather taut as they form during the relaxation stage (answering the questions why ordered regions formed during relaxation stage exhibit near perfect orientation and why they do not form in a disoriented state). Beyond the birefringence minimum, the expected crystallites of lower orientation eventually form with improved order.

Figure 14 shows the detailed structural development for LPEN stretched to strain of 80%. Following the stoppage of the stretching the birefringence remains constant in the early stages

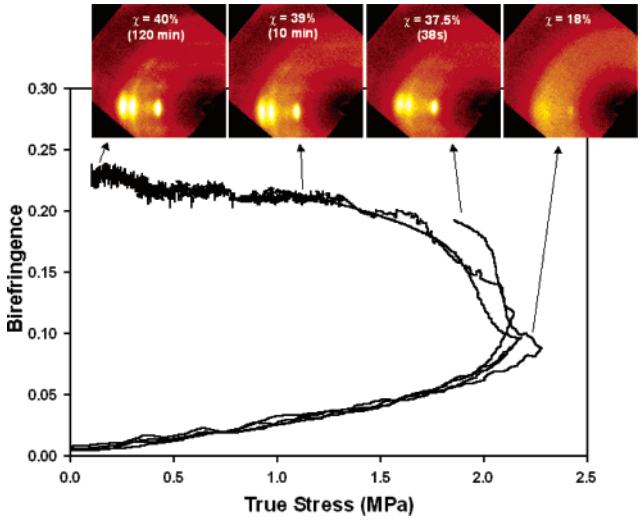

Figure 15. Detailed mechanooptical behavior and WAXD patterns of LPEN strain at 90% and relaxed for 2 h.

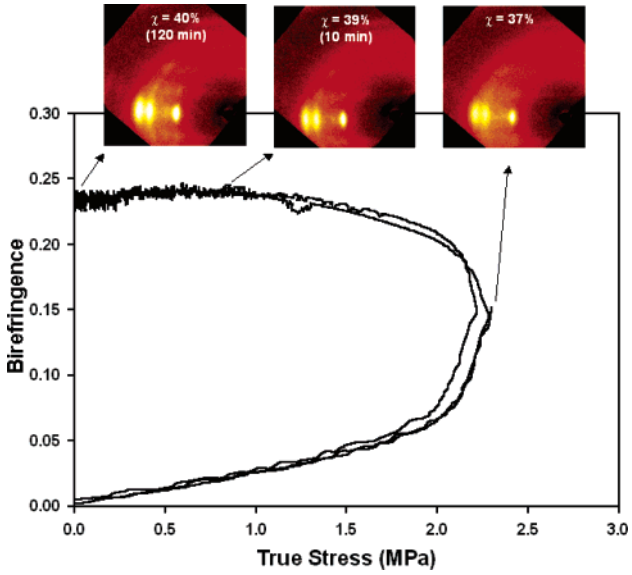

Figure 16. Detailed mechanooptical behavior and WAXD patterns of LPEN strain at 100% and relaxed for 2 h.

of relaxation while stress decays. In this case, the birefringence holds constant for a very short period of time and then starts increasing until the end of relaxation process. The rate of birefringence increase approaches a plateau as the relaxation proceeds to long times. At the end of the relaxation stage the off equatorial peaks become visible, indicating the establishment of three-dimensional order. However, the orientation of these crystalline regions also decline from near perfectly oriented state first observed at 44 s relaxation with 17% crystallinity with equatorial WAXD α(010).

At the start of relaxation within regime II there already are highly oriented—albeit containing considerable translational disorder—crystalline domains, as shown in Figure 15 and Figure 16. These two cases correspond to deformations between 90% and 100%, respectively. The initial plateau observed in the birefringence at the early stage of relaxation eventually disappears at 100% prestrained samples where birefringence begins to increase as soon as the stretching stage is terminated. At this point the material reached a crystalline state where three-dimensional ordering starts to form, as diffused off equatorial peaks appear while the overall crystalline orientation declines. This clearly follows earlier observations that the crystalline

regions that develop during the relaxation stage consist of chains of lower orientation partly as a result of relaxation processes. We do not think that the ordered regions that exhibit very highly oriented domains disorient during relaxation simply those that form at a later stage exhibit lower orientation, thereby reducing the total orientation of these regions.

In the second case, Figure 16, the relaxation causes an increase of structural ordering in the material with decrease of orientation as the relaxation time increases. The crystallinity increases from 37% after stretching to 40% after 2 h relaxation.

As alluded to earlier, the behavior shown in Figure 13 identifies the beginning of the network formation that, once started, arrests the decline of birefringence as the stress declines (see Figure 9) and has the strength of developing further if enough time is allowed. If one recalls (see Figure 2), the strain steadily increases during the total time of 2 h relaxation, explaining the increase of crystallinity observed. In this particular case, the increase of strain is motivated by a process of spontaneous deformation starting during the process of relaxation, in contrast to the other cases, where the deformation starts during the stretching process and continues/ends during the relaxation.

Network Formation. Both during the stretching process and during the relaxation, there are the same mechanistic evidences for the formation of a network. It occurs in the transition from regime I to regime II where the stress−optical rule starts deviating from the linearity and crystalline order first begins to take shape. First, there is an increase of orientation of the amorphous regions, as observed by the increase of birefringence together with the movement of T_{cc} to lower temperatures, maintaining the same crystallinity level. Further stretching encourages the formation of extremely high oriented ordered regions of poor translational ordering sprinkled throughout the sea of chains of varying orientation levels. During relaxation, the same structure is observed after a certain period of time, together with the reduction of orientation of the amorphous regions due to relaxation.

The molecular interpretation given to these results is as follows: during stretching within regime I, the applied deformation is transmitted affinely to the chains, which proves the chains are connected to each other by, at least, the entanglement node existing in the structure. The orientation is promoted and must be higher close to those nodes, since the chains are arrested between them and cannot move freely to rearrange themselves back to the random coil state, remaining in a stretched position. A simple schematic representation of this idea is shown in Figure 17.

According to the WAXD patterns, the chains are very highly oriented, but they are not properly aligned with each other to crystallize (Figure 17b). Nevertheless, the lowering of the entropy in these sites favors the rapid crystallization of the material. Either by further stretching or by relaxation, spontaneous deformation takes place causing the crystallization of the material in the regions of high orientation, arresting the chains permanently in the network, as depicted in Figure 18. The result is the birefringence increase with further stretching or relaxation accompanied by an increase in the crystallinity of the material. This confirms a similar model was also put forth by Peszkin et al.[29] on their investigations of heat treatment of preoriented fiber.

When network starts forming, it develops very quickly, tightening up with the crystallization of the material. Once the network is fully formed, it starts a process of "network deformation" which is made much harder due to increased crystallinity and taut connectivity. During relaxation, the chains of the amorphous regions within the crystalline sites (nodes of the network) are allowed to relax but only to a limited extent since the network arrests them. This is shown in Figures 3 and 15 by the lower change in stress upon relaxation when high strains are applied to the material.

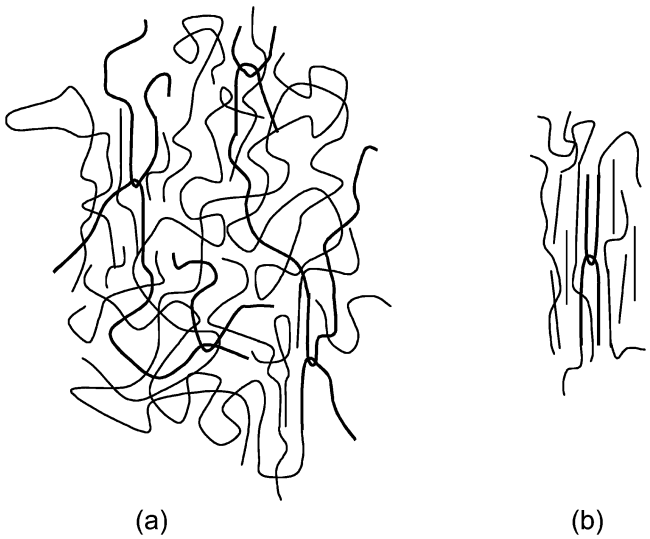

Figure 17. Schematic representation of network formation.

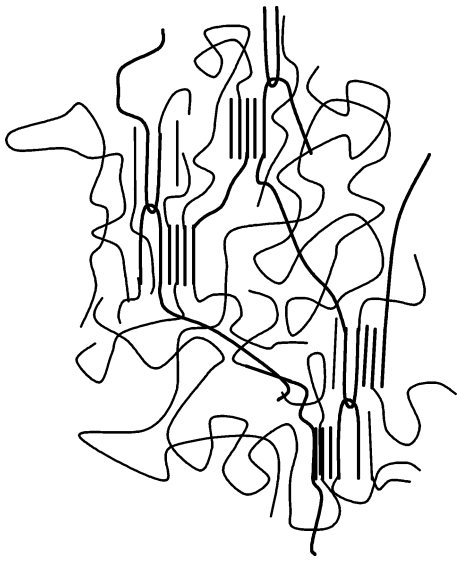

Figure 18. Schematic representation of network formation (connected taut chains forming the long-range network are indicated with darker lines).

Conclusions

The relaxation behavior of uniaxially oriented PEN in the rubbery state was investigated. It was found that relaxation behavior greatly depends on the state of the structure of the material at the start of relaxation. If the material is in the amorphous state, anywhere in regime I where the stress−optical rule is linear, the relaxation proceeds with a decrease in both the stress and birefringence due to the absence of long-range connectivity between the chains, allowing them to relax freely. Once deviation from linearity occurs, stress relaxation is accompanied by first a decrease in birefringence that then changes its trend and starts to increase. The increase of birefringence is proven to be due to a spontaneous deformation process developing during relaxation, which is accompanied by the formation of a very highly oriented structure, believed to be the starting point for the formation of the network. Well within regime II the birefringence increases very rapidly while

the stress decreases. In this regime, the strain rate is observed to be very high when relaxation starts, revealing that a continuous process of spontaneous deformation that starts during stretching and ceases during the relaxation period causes the increase of birefringence. In regime III, the stress decreases during relaxation but is accompanied by very little change in the birefringence. This result shows that when the network structure is well developed, it becomes structurally "muscle bound" by the developed crystallites and taut chains crisscrossing the body of the structure, preventing any further changes including crystallization and relaxation to take place.

Acknowledgment. We thank Portugese Government for the financial support of C.M. during her Ph.D. Program at University of Akron.

References and Notes

(1) Blundell, D. J.; Mahendrasingam, A.; Martin, C.; Fuller, W.; Mackerron, D. H.; Harvie, J. L.; Oldman, R. L.; Riekel, C. *Polymer* **2000**, *41*, 7793.
(2) Osborn, K. R.; Jenkins, W. A. *Plastic Films—Technology and Packaging Applications*; Technomic Publishing Co. Inc.: Lancaster, 1992; ISBN 87762-843-2.
(3) Cakmak, M.; Wang, Y. D.; Simhambhatla, M. *Polym. Eng. Sci.* **1990**, *30*, 721−733.
(4) Murakami, S.; Nishikawa, Y.; Tsuji, M.; Kawaguchi, A.; Kohjiya, S.; Cakmak, M. *Polymer* 1995, *36*, 291−297.
(5) Cakmak, M.; Lee, S. W. *Polymer* **1995**, *36*, 4039−4054.
(6) Murakami, S.; Yamakawa, T.; Tsuji, M.; Kohjiya, S. *Polymer* **1996**, *37*, 3945−3950.
(7) Cakmak, M.; Kim, J. C. *J. Appl. Polym. Sci.* **1997**, *64*, 729−747.
(8) Galay, J.; Cakmak, M. *J. Polym. Sci., Part B: Polym. Phys.* **2001**, *39*, 1107−1121.
(9) Blanton, T. N. *Powder Diffraction* **2002**, *17*, 125−131.
(10) Ito, H.; Suzuki, K.; Kikutani, T.; Nakayama, K. *PPS 18 Conf. Proc.*, Portugal, 2002.
(11) Schoukens, G.; Verschuere, M. *Polymer* **1999**, *40*, 3753−3761.
(12) Schoukens, G.; Samyn, P.; Maddens, S.; Van Audenaerde, T. *J. Appl. Polym. Sci.* **2003**, *87*, 1462−1473.
(13) Bhushan, B.; Jayantha-Rao, R. *J. Appl. Polym. Sci.* **2004**, *91*, 78−88.
(14) Martins, C.; Cakmak, M. *Macromolecules* **2005**, *38*, 4260−4273.
(15) Ryu, D. S.; Inoue, T.; Osaki, K. *Polymer* **1998**, *39*, 2515−2520.
(16) Pearce, R.; Cole, K. C.; Ajji, A.; Dumoulin, M. M. *Polym. Eng. Sci.* **1997**, *37*, 1795−1800.
(17) Oultache, A. K.; Kong, X.; Pellerin, C.; Brisson, J.; Pézolet, M.; Prud'homme, R. E. *Polymer* **2001**, *42*, 9051−9058.
(18) Matthews, R. G.; Ajji, A.; Dumoulin, M. M.; Prud'homme, R. E. *Polymer* **2000**, *41*, 7139−7145.
(19) Nobbs, J. H.; Bower, D. I.; Ward, I. M. *Polymer* **1976**, *17*, 25−36.
(20) Terada, T.; Sawatari, C.; Chigono, T.; Matsuo, M. *Macromolecules* **1982**, *15*, 998.
(21) Gupta, V. B.; Radhakrishnan, J.; Sett, S. K. *Polymer* **1993**, *34*, 3814−3822.
(22) Koike, Y.; Cakmak, M. *Polymer* **2003**, *44*, 4249−4260.
(23) Serhatkulu, T.; Cakmak, M. *SPE ANTEC Conf. Proc.* **1999**, 1645−1649.
(24) Toki, S.; Valladares, D.; Sen, T. Z.; Cakmak, M. *SPE ANTEC Conf. Proc.* **2001**, 1830−1834.
(25) Valladares, D.; Toki, S.; Sen, T. Z.; Yalcin, B.; Cakmak, M. *Macromol. Symp.* **2002**, *185*, 149−166.
(26) Koike, Y.; Cakmak, M. *Polymer* **2003**, *44*, 4249−4260.
(27) Cheng, S. Z. D.; Wunderlich, B. *Macromolecules* **1988**, *21*, 789−797.
(28) Biangardi, H. J.; Zachmann, H. G. *Prog. Colloid Polym. Sci.* **1977**, *62*, 71.
(29) Peszkin, P. N.; Schultz, J. M.; Lin, J. S. *J. Polym. Sci. Phys.* **1986**, *24*, 2591.

MA0522155